Enhanced 1.54 μm emission in Y-Er disilicate thin films on silicon photonic crystal cavities

R. Lo Savio,[1,*] M. Miritello,[2] A. Shakoor,[3] P. Cardile,[2] K. Welna,[3] L. C. Andreani,[1] D. Gerace,[1] T. F. Krauss,[3] L. O'Faolain,[3] F. Priolo,[2] and M. Galli[1]

[1]*Dipartimento di Fisica, Università di Pavia, Via Bassi 6, 27100 Pavia, Italy*
[2]*MATIS-IMM CNR and Dipartimento di Fisica e Astronomia, Università di Catania, via S. Sofia 64, 95123 Catania, Italy*
[3]*SUPA, School of Physics and Astronomy, University of St. Andrews, Fife KY16 9SS, St. Andrews, UK*
[*]*roberto.losavio@unipv.it*

Abstract: We introduce an Y-Er disilicate thin film deposited on top of a silicon photonic crystal cavity as a gain medium for active silicon photonic devices. Using photoluminescence analysis, we demonstrate that Er luminescence at 1.54 μm is enhanced by coupling with the cavity modes, and that the directionality of the Er optical emission can be controlled through far-field optimization of the cavity. We determine the maximum excitation power that can be coupled into the cavity to be 12 mW, which is limited by free carrier absorption and thermal heating. At maximum excitation, we observe that nearly 30% of the Er population is in the excited state, as estimated from the direct measurement of the emitted power. Finally, using time-resolved photoluminescence measurements, we determine a value of 2.3 for the Purcell factor of the system at room temperature. These results indicate that overcoating a silicon photonic nanostructure with an Er-rich dielectric layer is a promising method for achieving light emission at 1.54 μm wavelength on a silicon platform.

OCIS codes: (160.5690) Rare-earth-doped materials; (230.5298) Photonic crystals; (230.0230) Optical devices; (260.3800) Luminescence.

References and links

1. J. M. Shainline and J. Xu, "Silicon as an emissive optical medium," Laser Photonics Rev. **1**(4), 334–348 (2007).
2. D. Liang and J. E. Bowers, "Recent progress in lasers on silicon," Nat. Photonics **4**(8), 511–517 (2010).
3. G. Franzò, F. Priolo, S. Coffa, A. Polman, and A. Carnera, "Room-temperature electroluminescence from Er-doped crystalline Si," Appl. Phys. Lett. **64**(17), 2235–2237 (1994).
4. G. Davies, "The optical properties of luminescent centres in silicon," Phys. Rep. **176**(3-4), 83–188 (1989).
5. W. L. Ng, M. A. Lourenço, R. M. Gwilliam, S. Ledain, G. Shao, and K. P. Homewood, "An efficient room-temperature silicon-based light-emitting diode," Nature **410**(6825), 192–194 (2001).
6. S. G. Cloutier, P. A. Kossyrev, and J. M. Xu, "Optical gain and stimulated emission in periodic nanopatterned crystalline silicon," Nat. Mater. **4**(12), 887–891 (2005).
7. H. Ennen, J. Schneider, G. Pomrenke, and A. Axmann, "1.54-μm luminescence of erbium-implanted III-V semiconductors and silicon," Appl. Phys. Lett. **43**(10), 943–945 (1983).
8. A. Polman, G. N. van den Hoven, J. S. Custer, J. H. Shin, R. Serna, and P. F. A. Alkemade, "Erbium in crystal silicon: optical activation, excitation, and concentration limits," J. Appl. Phys. **77**(3), 1256–1262 (1995).
9. S. Coffa, G. Franzò, F. Priolo, A. Polman, and R. Serna, "Temperature dependence and quenching processes of the intra-4f luminescence of Er in crystalline Si," Phys. Rev. B Condens. Matter **49**(23), 16313–16320 (1994).
10. M. Miritello, R. Lo Savio, P. Cardile, and F. Priolo, "Enhanced down conversion of photons emitted by photoexcited $Er_xY_{2-x}Si_2O_7$ films grown on silicon," Phys. Rev. B **81**(4), 041411 (2010).
11. M. Miritello, R. Lo Savio, F. Iacona, G. Franzò, A. Irrera, A. M. Piro, C. Bongiorno, and F. Priolo, "Efficient luminescence and energy transfer in erbium silicate thin films," Adv. Mater. **19**(12), 1582–1588 (2007).
12. K. Suh, M. Lee, J. S. Chang, H. Lee, N. Park, G. Y. Sung, and J. H. Shin, "Cooperative upconversion and optical gain in ion-beam sputter-deposited $Er_xY_{2-x}SiO_5$ waveguides," Opt. Express **18**(8), 7724–7731 (2010).
13. Y. Yin, W. J. Xu, F. Wei, G. Z. Ran, G. G. Qin, Y. F. Shi, Q. G. Yao, and S. D. Yao, "Room temperature Er^{3+} 1.54 μm electroluminescence from Si-rich erbium silicate deposited by magnetron sputtering," J. Phys. D Appl. Phys. **43**, 335102 (2010).
14. S. Iwamoto, Y. Arakawa, and A. Gomyo, "Observation of enhanced photoluminescence from silicon photonic crystal nanocavity at room temperature," Appl. Phys. Lett. **91**(21), 211104 (2007).

#181504 - $15.00 USD Received 11 Dec 2012; revised 8 Mar 2013; accepted 15 Mar 2013; published 18 Apr 2013

15. M. Fujita, Y. Tanaka, and S. Noda, "Light emission from silicon in photonic crystal nanocavity," IEEE J. Sel. Top. Quantum Electron. **14**(4), 1090–1097 (2008).
16. R. Lo Savio, S. L. Portalupi, D. Gerace, A. Shakoor, T. F. Krauss, L. O'Faolain, L. C. Andreani, and M. Galli, "Room-temperature emission at telecom wavelengths from silicon photonic crystal nanocavities," Appl. Phys. Lett. **98**(20), 201106 (2011).
17. A. Shakoor, R. Lo Savio, P. Cardile, S. L. Portalupi, D. Gerace, K. Welna, S. Boninelli, G. Franzò, F. Priolo, T. F. Krauss, M. Galli, and L. O'Faolain, "Room temperature all-silicon photonic crystal nanocavity light emitting diode at sub-bandgap wavelengths," Laser Photonics Rev. **7**(1), 114–121 (2013).
18. M. Galli, A. Politi, M. Belotti, D. Gerace, M. Liscidini, M. Patrini, L. C. Andreani, M. Miritello, A. Irrera, F. Priolo, and Y. Chen, "Strong enhancement of Er^{3+} emission at room temperature in silicon-on-insulator photonic crystal waveguides," Appl. Phys. Lett. **88**(25), 251114 (2006).
19. T. J. Kippenberg, J. Kalkman, A. Polman, and K. J. Vahala, "Demonstration of an erbium-doped microdisk laser on a silicon chip," Phys. Rev. A **74**(5), 051802 (2006).
20. J. Kalkman, A. Tchebotareva, A. Polman, T. J. Kippenberg, B. Min, and K. J. Vahala, "Fabrication and characterization of erbium-doped toroidal microcavity lasers," J. Appl. Phys. **99**(8), 083103 (2006).
21. H.-S. Hsu, C. Cai, and A. M. Armani, "Ultra-low-threshold Er:Yb sol-gel microlaser on silicon," Opt. Express **17**(25), 23265–23271 (2009).
22. Y. Gong, M. Makarova, S. Yerci, R. Li, M. J. Stevens, B. Baek, S. W. Nam, L. Dal Negro, and J. Vuckovic, "Observation of Transparency of Erbium-doped Silicon nitride in photonic crystal nanobeam cavities," Opt. Express **18**(13), 13863–13873 (2010).
23. Y. Gong, M. Makarova, S. Yerci, R. Li, M. J. Stevens, B. Baek, S. W. Nam, R. H. Hadfield, S. N. Dorenbos, V. Zwiller, J. Vuckovic, and L. Dal Negro, "Linewidth narrowing and Purcell enhancement in photonic crystal cavities on an Er-doped silicon nitride platform," Opt. Express **18**(3), 2601–2612 (2010).
24. Y. Akahane, T. Asano, B. S. Song, and S. Noda, "High-Q photonic nanocavity in a two-dimensional photonic crystal," Nature **425**(6961), 944–947 (2003).
25. S. L. Portalupi, M. Galli, C. Reardon, T. F. Krauss, L. O'Faolain, L. C. Andreani, and D. Gerace, "Planar photonic crystal cavities with far-field optimization for high coupling efficiency and quality factor," Opt. Express **18**(15), 16064–16073 (2010).
26. C. P. Reardon, I. H. Rey, K. Welna, L. O'Faolain, and T. F. Krauss, "Fabrication and characterization of photonic crystal slow light waveguides and cavities," J. Vis. Exp. (69): e50216 (2012), doi:10.3791/50216.
27. R. Lo Savio, M. Miritello, A. M. Piro, F. Priolo, and F. Iacona, "The influence of stoichiometry on the structural stability and on the optical emission of erbium silicate thin films," Appl. Phys. Lett. **93**(2), 021919 (2008).
28. M. Galli, S. L. Portalupi, M. Belotti, L. C. Andreani, L. O'Faolain, and T. F. Krauss, "Light scattering and Fano resonances in high-Q photonic crystal nanocavities," Appl. Phys. Lett. **94**(7), 071101 (2009).
29. P. C. Becker, N. A. Olsson, and J. R. Simpson, *Erbium-Doped Fiber Amplifiers: Fundamentals and Technology* (Academic, 1999)
30. M. El Kurdi, X. Checoury, S. David, T. P. Ngo, N. Zerounian, P. Boucaud, O. Kermarrec, Y. Campidelli, and D. Bensahel, "Quality factor of Si-based photonic crystal L3 nanocavities probed with an internal source," Opt. Express **16**(12), 8780–8791 (2008).
31. G. N. van den Hoven, E. Snoeks, A. Polman, C. van Dam, J. W. M. van Uffelen, and M. K. Smit, "Upconversion in Er-implanted Al_2O_3 waveguides," J. Appl. Phys. **79**(3), 1258–1266 (1996).
32. M. Miritello, P. Cardile, R. Lo Savio, and F. Priolo, "Energy transfer and enhanced 1.54 μm emission in erbium-ytterbium disilicate thin films," Opt. Express **19**(21), 20761–20772 (2011).
33. E. M. Purcell, "Spontaneous emission probabilities at radio frequencies," Phys. Rev. **69**, 681–681 (1946).
34. E. Snoeks, P. G. Kik, and A. Polman, "Concentration quenching in erbium implanted alkali silicate glasses," Opt. Mater. **5**(3), 159–167 (1996).
35. M. J. Weber, "Radiative and multiphonon relaxation of rare-earth ions in Y_2O_3," Phys. Rev. **171**(2), 283–291 (1968).
36. W. Fowler and D. Dexter, "Relation between absorption and emission probabilities in luminescent centers in ionic solids," Phys. Rev. **128**(5), 2154–2165 (1962).
37. C. Creatore, L. C. Andreani, M. Miritello, R. Lo Savio, and F. Priolo, "Modification of erbium radiative lifetime in planar silicon slot waveguides," Appl. Phys. Lett. **94**(10), 103112 (2009).
38. L. C. Andreani, G. Panzarini, and J. M. Gerard, "Strong-coupling regime for quantum boxes in pillar microcavities: Theory," Phys. Rev. B **60**(19), 13276–13279 (1999).
39. M. Notomi, "Manipulating light with strongly modulated photonic crystals," Rep. Prog. Phys. **73**(9), 096501 (2010).
40. J. M. Gérard, "Solid-State Cavity-Quantum Electrodynamics with Self-Assembled Quantum Dots," Top. Appl. Phys. **90**, 269–314 (2003).
41. G. L. J. A. Rikken and Y. A. R. R. Kessener, "Local field effects and electric and magnetic dipole transitions in dielectrics," Phys. Rev. Lett. **74**(6), 880–883 (1995).
42. Q. Xu, V. R. Almeida, R. R. Panepucci, and M. Lipson, "Experimental demonstration of guiding and confining light in nanometer-size low-refractive-index material," Opt. Lett. **29**(14), 1626–1628 (2004).

1. Introduction

Light emission from silicon is one of the main challenges of the silicon photonics paradigm, due to the material's indirect band gap. Great efforts have been made in the last decades to

#181504 - $15.00 USD Received 11 Dec 2012; revised 8 Mar 2013; accepted 15 Mar 2013; published 18 Apr 2013

overcome this limit and to fabricate Si light emitters; defect and device engineering are among the most interesting approaches [1,2].

Defect engineering consists of the intentional insertion of optically active impurities, such as dopants or defects [3–6], into the crystalline silicon (c-Si). In particular, since the first demonstration of optical emission from Er-doped Si in 1983 [7], erbium has been widely studied as the active impurity. The transition between the first excited state and the ground state gives rise to the emission of a photon at the technologically important wavelength of 1.54 μm. Er-doped crystalline silicon as a luminescent material has two main drawbacks, however: (i) the low solubility of Er in Si limits the maximum concentration to about 10^{18} Er/cm^3, and (ii) the luminescence is strongly quenched at room temperature [8,9]. These limits can be overcome by introducing the Er atoms into different hosts that are compatible with Si, and that can accommodate higher Er concentrations. For example, Y-Er disilicate ($Y_{2-x}Er_xSi_2O_7$, $0 < x \leq 2$) is a good host candidate since it affords a maximum solubility of 10^{22} cm^{-3}. This high solubility is due to the fact that both constituent materials ($Er_2Si_2O_7$, and $Y_2Si_2O_7$) have the same crystalline structure with very similar lattice parameters, and both Er and Y atoms occupy the same atomic sites [10]. In addition Y is optically inactive and the optical properties depend entirely on Er. Internal gain in a ridge waveguide and electroluminescence have already been demonstrated in these compounds [11–13], which encourages further developments.

The device engineering approach consists of the optical emission enhancement via the strong confinement of electromagnetic fields in a small volume that contains the optically active centers. For example, light emission enhancement in crystalline Si photonic crystal (PhC) cavities was demonstrated as a combination of the Purcell effect and the increase of the extraction efficiency [14–17]. This approach has also been used successfully to enhance the optical emission of Er atoms by coupling them with photonic crystals [18] and high-Q optical cavity modes, such as microdisks [19] and microtoroids [20,21]; stimulated emission and linewidth narrowing have also been observed [22,23]. All of these results were realised in insulating materials, however, and not in silicon; moreover, the active atoms had a maximum concentration limited by the typical values of Er doping in insulators- of the order of 10^{20} at/cm^3.

In this study, we combine both approaches and couple the 1.54 μm emission of Er atoms with the optical modes of an L3 silicon PhC cavity by depositing a very thin Y-Er disilicate layer (≈10 nm) on top of the photonic structure. Our approach presents two main advantages: (i) the novel active material allows us to fine-control the Er concentration, with the possibility of increasing the number of emitting atoms up to the maximum concentration of 10^{22} at/cm^3; (ii) the photonic structures are fully fabricated in crystalline silicon, allowing us to create high quality factor and small volume cavities. We demonstrate an enhancement of the Er emission due to the coupling with the cavity fundamental modes and show that the maximum Er concentration in the excited state is about 30%.

2. Samples design and fabrication

The photonic structures studied here are L3 cavities, formed in a PhC slab by removing three holes from the Γ-K direction of a triangular lattice. The lattice constant (a) was varied between 405 and 430 nm in steps of 1 nm to fine-tune the cavity resonance wavelength, while the hole radius (r) was kept at fixed ratio r/a = 0.275. This wide parameter-range was chosen to tune the fundamental cavity mode around 1.54 μm and to allow for the modification of the resonance wavelength induced by the deposition of the silicate thin film. The two holes closest to the cavity in the Γ-K direction (circled in blue in Fig. 1(b) below) were shrunk and displaced in order to increase the cavity quality factor (Q-factor) [24]. Moreover, we applied the far-field optimization technique to improve out-of-plane coupling [25], by modifying the radius of the holes close to the cavity (see larger holes circled in red in Fig. 1(b) below). In particular, if we define Δr as the radius modification, cavities with Δr = 0, + 6, and + 21 nm were fabricated with the Δr = 0 nm devices acting as a reference. In principle, since we keep r/a fixed in the lithographic tuning, we should also scale Δr with the lattice constant –

#181504 - $15.00 USD Received 11 Dec 2012; revised 8 Mar 2013; accepted 15 Mar 2013; published 18 Apr 2013

however, since the relative variation is only a few percent and is below the resolution of the lithography, for simplicity we keep Δr fixed.

Photonic crystal lattices of 10 × 10 μm^2 size were fabricated by e-beam lithography and reactive ion etching on a SOI substrate (220 nm thick c-Si on top of 2000 nm thick SiO_2). Afterwards the oxide layer underneath the PhC slab was removed by HF to form a free-standing membrane, see [26] for more details.

The structures were then coated by a 10 nm thick Y-Er disilicate film. The film was deposited by magnetron sputtering in an ultra-high-vacuum chamber by co-sputtering from Y_2O_3, Er_2O_3, and SiO_2 targets arranged in a confocal geometry. During the deposition, the substrate was heated to 400 °C. Following deposition, the samples were annealed at 1250 °C for 30 seconds in an O_2 ambient to induce crystallization of the film and to improve the optical emission at 1.54 μm through the reduction of non-radiative decay channels [11,27].

The film composition was evaluated by Rutherford Backscattering Spectrometry, confirming that the deposited film had a disilicate-like stoichiometry ([Y + Er]:[Si]:[O] = 2:2:7), with an Er concentration of 8 × 10^{20} Er/cm^3 (corresponding to 1.2 at.%). A schematic cross-section view of the final device is shown in Fig. 1(a), while a scanning electron micrograph of a finished L3 cavity is shown in Fig. 1(b). The Si membrane is intact, even after the high-T annealing.

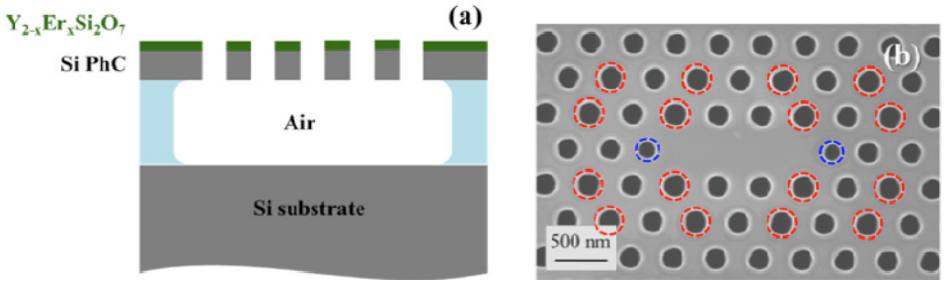

Fig. 1. (a) Cross-section scheme of the top-coated Si PhC membrane. (b) Scanning electron microscopy image of a top-coated L3 cavity, after the Y-Er disilicate deposition and following thermal treatment. Blue-dashed circles indicate the holes shrunk and displaced to increase the Q-factor, while red-dashed circles indicate the holes enlarged by Δr to enhance the far-field vertical coupling.

3. Photoluminescence analysis

3.1 Er coupling with L3 cavity modes

Er emission from bare SOI material and from L3 cavities was measured at room temperature by using a confocal micro-photoluminescence (μPL) setup. Er atoms were resonantly excited by a diode laser operating at 980 nm and focused to a spot of about 1 μm diameter by a high numerical aperture (NA = 0.8) microscope objective. The relative position between the laser spot and the sample was controlled with piezoelectric nanopositioners. The emission is collected through the same objective and sent to an InGaAs detector equipped with two diffraction grating monochromators to afford different spectral resolutions.

The pump laser has a wavelength resonant with the $^4I_{15/2} \rightarrow {}^4I_{11/2}$ transition of Er; the excited atoms quickly undergo the non-radiative transition to $^4I_{13/2}$, and then radiatively de-excite to the ground state $^4I_{15/2}$ with the emission of photons at a wavelength around 1.54 μm. The PL emission observed in Y-Er disilicate film deposited on the unpatterned SOI substrate is shown as a dashed black line in Fig. 2(a). The lineshape is typical for Er disilicates crystallized in the α-phase; among the different possible crystalline phases of this material, the α-phase shows the highest PL intensity due to its longer lifetime [10,27].

When the excitation spot is moved to the center of the L3 cavity, the PL spectrum consists of a sharp peak, corresponding to the excitation of the fundamental cavity mode, superimposed on a weaker background, corresponding to the PL emission of the Er atoms in

#181504 - $15.00 USD Received 11 Dec 2012; revised 8 Mar 2013; accepted 15 Mar 2013; published 18 Apr 2013

the disilicate layer coating the L3 cavity. PL spectra of far-field optimized cavities (having Δr = + 6 nm) with different lattice constants are shown in Fig. 2(a). The most intense peaks, between 1525 and 1560 nm, correspond to the fundamental cavity modes. The modes shift towards longer wavelength with increasing lattice constant, and their intensities roughly follow the PL shape of Er in disilicate film, shown as a dashed black line in the same figure.

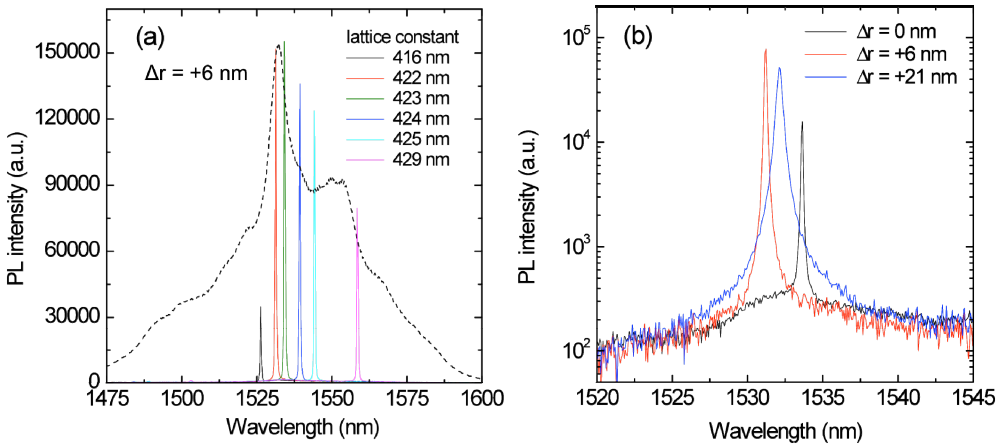

Fig. 2. PL emission from top-coated L3 cavities by varying (a) the lattice parameter and (b) the far-field optimization parameter. The dashed black line in (a) is the shape of PL observed in the Y-Er disilicate film.

The effect of the far-field optimization is clearly apparent in Fig. 2(b), where we show the PL spectra of three cavities with different Δr, that feature modes which are resonant with the Er emission peak. As expected, the PL of the far-field optimized cavities with $\Delta r \neq 0$ is more intense because of the higher coupling efficiency into the collection cone of the microscope objective. At the same time, the peaks are broader by increasing Δr as a consequence of the reduced Q-factor [25]. However PL analysis is not the most accurate technique to measure high-Q factor cavities, since the maximum value is limited to about 15000, due to the spectral resolution of the diffraction gratings. Therefore their values were measured using the resonant scattering technique [28] (data not shown), yielding Q = 26000, 16200, and 4000 for Δr = 0, + 6, and + 21 nm, respectively. The Q-factors of the far-field optimized cavities are comparable with the values measured before the coating process, while a 2-fold decrease is observed for the higher Q-factor reference structure (Δr = 0 nm), where the higher optical losses induced by the disilicate are more apparent. Therefore, the coating layer does not appear to have a detrimental effect on the Q-factor of the far-field optimized cavities. The PL emission is enhanced by about two orders of magnitude in all the investigated samples, as estimated by the peak-to-background ratios in Fig. 2(b). This is due to a combination of the increased extraction efficiency given by the presence of the photonic crystal pattern, and the Purcell effect given by the coupling with the cavity modes. We note that this enhancement, is comparable to the best values from L3 PhC cavities reported previously [14,16]. Finally the structure with Δr = + 6 nm exhibits the strongest PL as a result of the best trade-off between the increased vertical coupling and the reduced Q-factor, and we only consider this in the following.

In order to exploit the very high Er concentrations allowed in this active material, it is necessary to excite the highest possible number of Er atoms. However, as high excitation powers are required, the effects of the interaction between the pump laser and the silicon slab must be evaluated. In fact, by considering an Er excitation cross section of 1×10^{-21} cm^2 [29], we estimate that only a fraction of 8×10^{-7} of the incoming photons are absorbed by Er in the top layer, while a much higher fraction (2×10^{-3}) are absorbed in the silicon slab. Figure 3(a) shows the normalized PL spectra observed at different excitation powers (the normalization factors are indicated in the legend). Up to 6 mW pump power the peak intensity increases and

#181504 - $15.00 USD Received 11 Dec 2012; revised 8 Mar 2013; accepted 15 Mar 2013; published 18 Apr 2013

the lineshape is almost unchanged; increasing the pump power further, the PL intensity saturates, and then even decreases. At the same time, a peak redshift and broadening occurs (blue curve and full squares in Fig. 3(a)). The former effect is due to sample heating, with the maximum observed cavity mode redshift (about 1 nm) corresponding to $\Delta T \approx 20$ °C; the latter is related to the absorption induced by free carriers created in silicon that induces a reduction of the cavity Q-factor [16,30]. Although both effects are a direct consequence of the interaction between the pump photons and the silicon slab, they also have a detrimental influence on the Er luminescence. The sample heating moves the resonance away from the maximum Er PL peak, and the Q-factor reduction is responsible for a less efficient Er-cavity interaction.

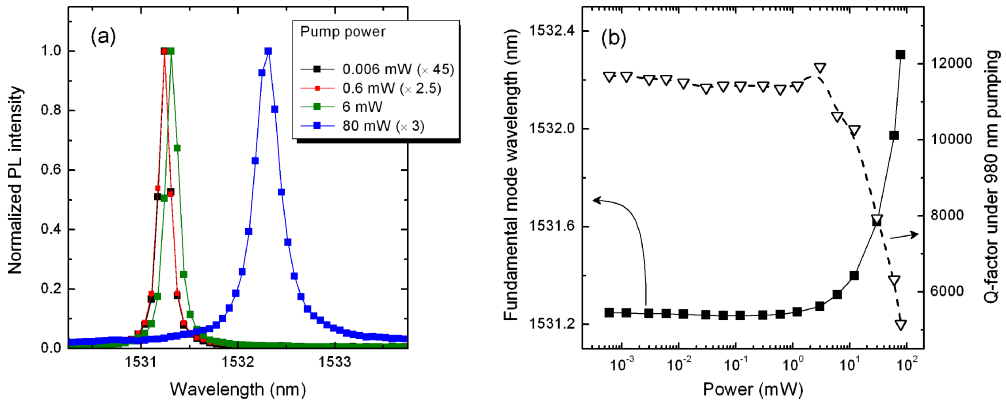

Fig. 3. (a) Normalized spectra of cavity mode PL for different pump powers; the normalization factors are indicated in the legend. (b) Trend of fundamental mode wavelength (full squares) and Q-factor (open triangles) for different pump powers.

Both effects explain the reduction of PL at the high pump power in Fig. 3(a). The peak PL wavelength and the Q-factor trends are plotted as a function of the pump power in Fig. 3(b). At low pump powers, the Q-factor is constant at about 12000, close to the resolution limit of the spectrometer. For $P > 12$ mW, a strong modification of both parameters occurs, setting an upper limit for the excitation power that can be used in this structure without the occurrence of these detrimental effects. This limit is strictly due to the photonic structure and it is not related to the active material that can sustain higher excitation powers. It could be overcome by using a 1480 nm exciting laser in order to completely suppress free carriers in the underlying membrane, but without a decrease of the efficiency of Er coupling, owing to the very similar Er excitation cross sections under the two excitation conditions [29].

3.2 Concentration of excited Er in cavity

The maximum power emitted by the cavity for excitation at 12 mW was measured with an InGaAs power meter coupled to a low-pass optical filter, thus excluding photons below 1500 nm not related to Er emission. The raw observed value of 15 pW was corrected taking into account the following factors.

Through the analysis of PL spectra we estimate that only the 75% of the emitted power comes from the Er coupled to the cavity mode (the remaining 25% was attributed to the background PL). The absorption loss of the acquisition line of the setup (31%) was evaluated by directly measuring the transmittance at 1540 nm of the dichroic mirrors and the optical filters. The absorption loss of the microscope objective (35%) was measured by directly measuring the transmission of a 1540 nm laser light. The fraction of light that can be collected by the microscope objective was evaluated through FDTD methods (by using commercial software from Lumerical Solutions), integrating the far-field profile emission over an angle corresponding to the collection angle of the objective [25], yielding about 60%.

#181504 - $15.00 USD Received 11 Dec 2012; revised 8 Mar 2013; accepted 15 Mar 2013; published 18 Apr 2013

Finally, only the photons emitted in the upper plane, that is the 50% of the total, can be collected by the objective, and then directly measured.

Following it, the estimated maximum power emitted by Er atoms coupled to the cavity mode is about 85 pW, over a very narrow peak ($\Delta\lambda$ = 0.15 nm). The trend of the emitted power as a function of incident pump power is shown in Fig. 4. If we consider the pump power absorbed by Er ions, the efficiency is 0.9% for 12 mW; but given the sub-linear trend, this value further increases at lower pump powers.

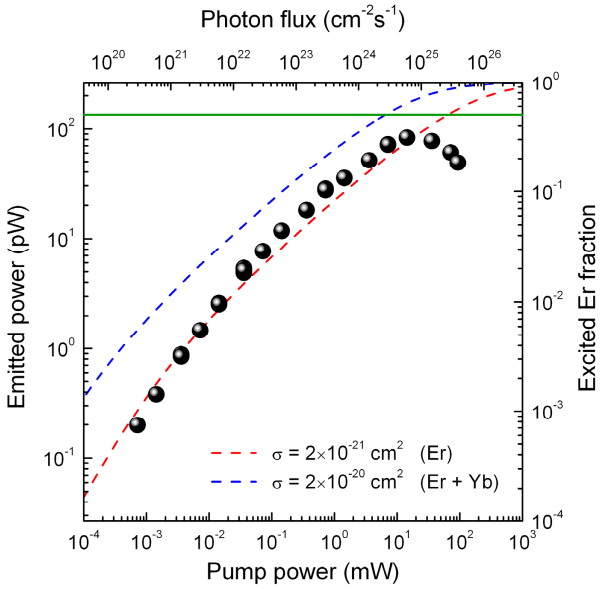

Fig. 4. PL emission vs pump power. The dashed red line is not a fit and is derived from Eq. (2). The dashed blue line is the calculated trend of the excited Er fraction in presence of Yb. The population inversion threshold is indicated as a green line.

Starting from the emitted power, we can estimate the concentration of excited Er as a function of pump power (right hand scale in Fig. 4). If we assume that each Er atom emits a power of ($1.3 \times 10^{-19}/\tau_{R,cav}$) W, with $\tau_{R,cav}$ the radiative lifetime of Er atoms coupled to the cavity mode, the total number of emitting dipoles is given by the ratio between the total emitted power and the power emitted by a single atom. We estimate a radiative lifetime of 4.0 ± 0.5 ms (see next paragraph for the details), so a maximum of $2.6 \pm 0.3 \times 10^6$ Er atoms are excited to achieve the 85 pW emission. If we assume a cavity mode area of 1 μm^2 and that Er atoms are coupled to the cavity mode throughout the entire film thickness of 10 nm, then there are $2.6 \pm 0.3 \times 10^{20}$ Er/cm^3 excited, about 32 ± 4% of the total number.

In order to check the reliability of our estimated values we calculate the excited Er fraction starting from the Er rate equations. In the pump power range we investigated, the PL trend is sub-linear, suggesting that up-conversion processes that deplete the first excited level are occurring [31]. The rate equation of the first excited Er level in the two-level approximation (i.e., by assuming that all Er atoms resonantly excited by the pump to the $^4I_{11/2}$ level relax to the $^4I_{13/2}$ instantaneously), including the up-conversion term, is as follows:

$$\frac{dN_1(t)}{dt} = \sigma\varphi\left(N_{Er} - N_1(t)\right) - \frac{N_1}{\tau} - C\left[N_1(t)\right]^2. \qquad (1)$$

$N_1(t)$ is the Er population in the excited $^4I_{13/2}$ level at the time t, σ is the excitation cross section (2×10^{-21} cm^2 according to Table 4.5 in ref [29].), φ is the pumping flux, N_{Er} is the Er atomic concentration and C is the up-conversion coefficient. Here τ represents the total lifetime of Er in cavity, including both radiative and non-radiative terms; it was

#181504 - $15.00 USD Received 11 Dec 2012; revised 8 Mar 2013; accepted 15 Mar 2013; published 18 Apr 2013

experimentally measured, being 2.1 ms (see next paragraph for more details). By considering the steady-state condition reached under a continuous-wave excitation pump, we obtain:

$$N_1(\varphi)=\frac{1}{2C\tau}\left[\sqrt{1+\sigma\varphi\tau\left(2+4CN_{Er}\tau+\sigma\varphi\tau\right)}-\left(1+\sigma\varphi\tau\right)\right]. \quad (2)$$

The only parameter we cannot directly measure is the up-conversion coefficient C; it can be extrapolated from the values reported in ref [10], giving $C = 1.3 \times 10^{-16}$ cm^3/s. Substituting all the parameters in Eq. (2) we can calculate the excited Er concentration as a function of the pumping flux; the resulting trend is the dashed red curve in Fig. 4. We achieved a good agreement with the experimental data, up to 12 mW, thus confirming our estimation of the excited Er concentration. Note that the PL decrease for P > 12 mW is attributed to the detrimental effects of the underlying Si photonic crystal.

Finally, while the maximum excited Er concentration obtained in this work corresponds to 30% of the entire Er population by considering the simulated trend of excited Er, it is evident that the population inversion threshold (50% of excited population) could be obtained for a pump power higher than 12 mW. However, detrimental effects due to the absorption of photons in Si slab, and not in the active medium, currently limit us to this value. This result is very encouraging as it demonstrates that by overcoming the limited excitation power, population inversion threshold can indeed be reached, making this approach very promising for the realization of optical gain at 1.54 μm. An increase of the maximum allowed power could be achieved by reducing the interaction between the Si slab below the active material and the pump photons, for example by using a 1480 nm excitation laser without influencing the efficiency of the Er-cavity mode interaction as observed in the previous paragraph.

Alternatively, the fraction of excited Er can also be increased by the replacement of optically inactive yttrium with ytterbium, determining an enhancement by one order of magnitude of the excitation cross section [21,32]. The calculated trend of excited Er fraction as a function of incident flux in presence of Yb is shown as a dashed blue line in Fig. 4; in this case, the population inversion threshold could be reached already at the maximum pump flux allowed by the photonic structure studied here.

4. Time-resolved photoluminescence and Purcell effect

The Er PL enhancement is only an indirect signature of the Purcell effect that occurs when Er atoms are coupled to a cavity mode; a direct proof requires measuring the change in lifetime [33]. We measured the lifetime at room temperature on a setup similar to that used for μPL. The exciting laser was mechanically chopped at 30 Hz to give a square-wave pump signal, and the collected light was sent to a superconducting single photon detector (SSPD) cooled to 4.2 K, that produces an output voltage each time a photon is absorbed. The lifetime is recorded via the time-correlated single photon counting technique.

Figure 5 shows two decay curves obtained under different conditions. The black curve represents the decay of the cavity resonance PL, obtained by spectrally selecting the narrow cavity peak only. The red curve is the time decay of the emission collected from Er atoms on the PhC lattice outside the cavity region; the signal was collected from a 1500-1800 nm transmission window.

#181504 - $15.00 USD Received 11 Dec 2012; revised 8 Mar 2013; accepted 15 Mar 2013; published 18 Apr 2013

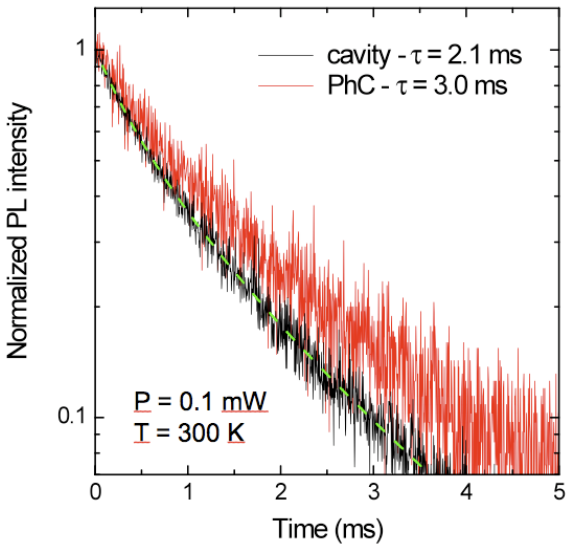

Fig. 5. Decay curves of fundamental cavity mode PL (black curve); PL collected from the PhC lattice outside the cavity region (red line). The dashed green line is the best fit of the black curve obtained by using Eq. (3).

At first glance, all of the curves show a non-single exponential behavior; we attribute this to the presence of up-conversion processes [31], although the decay curves were acquired at the lowest possible pump power in order to reduce the Er-Er interactions as much as possible. In order to extract the lifetime values, the experimental curves must then be fitted by using the solution of Eq. (1), when the external pump is switched off (corresponding to the case $\sigma = 0$).

$$\frac{I_1(t)}{I(0)} = \frac{1}{(1+N_1(0)C\times\tau)e^{t/\tau} - N_1(0)C\times\tau}. \tag{3}$$

In this case the fitting parameters are the lifetime τ, and the product $N_1(0)C$ between the excited Er concentration when the laser is switched-off and the up-conversion coefficient. From Fig. 5, the corresponding lifetime of Er atoms coupled to the cavity mode is the shortest (2.1 ms); if we move the laser spot away from the cavity region into the PhC lattice, the lifetime is increased to 3.0 ms. The decay rate for Er in PhC is given by the reciprocal sum of radiative (R) and non-radiative (nR) lifetime:

$$\left(\frac{1}{\tau}\right)_{PhC} = \frac{1}{\tau_R} + \frac{1}{\tau_{nR}}. \tag{4}$$

The radiative decay rate of Er in cavity is increased by the Purcell effect through the Purcell factor F_P, and Eq. (4) is modified into:

$$\left(\frac{1}{\tau}\right)_{cav} = F_P\frac{1}{\tau_R} + \frac{1}{\tau_{nR}}. \tag{5}$$

Then, in order to estimate the F_P values in our system we can compare the lifetime of Er in cavity and in PhC, supposing that non-radiative lifetime is the same in both cases. This is true since the main non-radiative decay channel in Er-containing insulating host is the concentration quenching due to Er-Er energy transfer [34]. This process depends only on the Er-Er mean distance and then it is not influenced by the dielectric environment.

#181504 - $15.00 USD Received 11 Dec 2012; revised 8 Mar 2013; accepted 15 Mar 2013; published 18 Apr 2013

$$F_P = \left[\left(\frac{1}{\tau}\right)_{cav} - \left(\frac{1}{\tau}\right)_{PhC}\right]\tau_R + 1. \quad (6)$$

Unfortunately it is not possible to estimate the radiative lifetime from the time decay measurements, since the Er concentration is too high to neglect non-radiative decay channels, such as concentration quenching [34]. Its value must be deduced following some approximations. As a starting point we consider the measured radiative lifetime of Er in a bulk Y_2O_3 (8 ms) [35]. The radiative lifetime of Er embedded in a homogeneous medium depends only on the refractive index of the host mateial, following an inverse squared dependence [36]; since the refractive indexes of the Y-Er disilicate film and Y_2O_3 are 1.77 and 1.9 respectively [10], then we estimate radiative lifetime of Er in disilicate to be 9 ms. Further modifications of the lifetime τ_R due to placing the disilicate on top of the Si layer, which reduces the lifetime by a factor of about 1.4 [37], and due to interaction of the Er emission with the photonic bandgap of the underlying PhC, which increases the lifetime by about the same amount, nearly compensate each other and lead to a small error bar in the estimation.

This finally gives us $F_P \approx 2.3 \pm 0.3$, comparable to that reported for a L3 PhC cavity fully fabricated in Er-doped silicon nitride [23]. This means that the radiative lifetime of the Er atoms coupled to the cavity mode ($\tau_{R,cav}$) is further reduced to 4 ms.

The spontaneous emission rate enhancement of a single dipole, spectrally and spatially matched to the electric field antinode of a generic photonic cavity, is ideally given by the well-known Purcell expression

$$F_{P,ideal} = \frac{3(\lambda/n)^3 Q}{4\pi^2 V_{eff}}. \quad (7)$$

where the effective cavity mode volume is consistently defined as [38–40]:

$$V_{eff} = \frac{\int \varepsilon(\mathbf{r})|\mathbf{E}(\mathbf{r})|^2 d\mathbf{r}}{\varepsilon(\mathbf{r_{max}})|\mathbf{E}(\mathbf{r_{max}})|^2}. \quad (8)$$

In the latter expression $\mathbf{r_{max}}$ is the position that maximizes the product $\varepsilon(\mathbf{r})|\mathbf{E}(\mathbf{r})|^2$. In our case, we can assume that the active medium is made of a uniformly distributed ensemble of narrow-line emitters. Indeed, the overall emission linewidth of Er atoms in insulating hosts is determined by inhomogenous or Stark splitting of the extremely narrow atomic transitions between the different multiplets involved in the $^4I_{13/2} \rightarrow {}^4I_{15/2}$ decay [29]. The long radiative lifetime, in the millisecond range, clearly supports this hypothesis. We can then assume that the emitter linewidth is much smaller than the cavity mode, and apply a generalized expression for the Purcell factor that only depends on the cavity Q-factor [40]:

$$F_P = \frac{3\lambda^3 Q}{4\pi^2 n \varepsilon_{max} V_{eff}} \int \frac{1}{3} p(\mathbf{r})|\mathbf{f}(\mathbf{r})|^2 d\mathbf{r}. \quad (9)$$

This expression fully takes into account the convolution of the spatial distribution function of the active dipoles, $p(\mathbf{r})$, with the cavity mode spatial profile, here consistently defined as $\mathbf{f}(\mathbf{r}) = \mathbf{E}(\mathbf{r})/|\mathbf{E}(\mathbf{r_{max}})|$, and where the factor 1/3 in the integral accounts for the random orientation of the dipole emitters. Although local-field effect may have an influence on the radiative lifetime in a dielectric medium, depending on the details of the local surrounding of the impurity [41], in the present case the local-field effects are implicitly included in the radiative lifetime of Er in the silicate matrix. Notice that the "local" surrounding is defined on a scale of a few lattice constants, and is unaffected by a material thickness of 10 nm: thus, the local-field effect gives no corrections to our measured or calculated Purcell factor.

#181504 - $15.00 USD Received 11 Dec 2012; revised 8 Mar 2013; accepted 15 Mar 2013; published 18 Apr 2013

To estimate the expected Purcell enhancement in our system we apply Eq. (9) to the L3 photonic crystal cavity corresponding to the measured device. The electric field profile is calculated with the FDTD method, by using commercial software from Lumerical Solutions. We assume uniformly distributed Er active centers on the surface of the cavity, with a layer thickness of 10 nm. The result is an estimated Purcell factor of $F_P \approx 3.2$, close to the experimentally determined value.

The relatively low Purcell factor as compared to the ideal value $F_{P,ideal}$ of Eq. (7) follows from three effects: (i) the polarization factor 1/3, as the Er emitter dipoles are randomly oriented; (ii) the uniform spatial distribution of the dipoles in the plane, instead of having dipoles at the cavity center; (iii) the non-optimal location of Er layer on top of the silicon slab, instead of having dipoles at the middle of the slab. All these effects are contained in the formula (9) and are taken into account in the FDTD evaluation of the Purcell factor. Effect (iii) could be overcome by fabricating similar PhC cavities in which the active material is placed inside the crystalline silicon, in order to improve the overlap between the active layer and the cavity region, by using e.g. vertical slot waveguides [42]: this solution would be especially advantageous, as it would also reduce the effective volume V_{eff} by the slot effect leading to enhanced electric fields in the slot region.

5. Conclusions

In summary, we have successfully demonstrated coupling between Er atoms and the optical modes of an L3 photonic crystal cavity realized in crystalline silicon by coating the cavity with a thin Y-Er disilicate layer. The PL of Er atoms in the cavity region is enhanced by the increased extraction efficiency and the Purcell effect, the extraction efficiency being maximized using far-field optimization. By measuring the emitted power, we estimate that 30% of Er population is excited; this opens the route for further improvements through an optimization of both active material and photonic structure. The Purcell factor that we extract from time-resolved photoluminescence measurements is $F_P \approx 2.3$, close to the calculated value of $F_P \approx 3.2$. However, we expect F_P to increase in optimized PhC cavities in which the active material can be inserted spatially closer to the region of highest field confinement. Finally since our photonic structure is fully fabricated in crystalline silicon and coated with a very thin insulating layer, it is possible, in principle, to fabricate an electroluminescent device. The Er atoms could be excited through an impact excitation mechanism, with carriers tunneling through the active layer, a scheme that has already been used to demonstrate electroluminescence in other silicate-based devices [13]. This would greatly broaden the range of applications for the present Si-based nanoemitters opening the route to the development of small-sized Er light source and amplifiers.

Acknowledgments

This work was supported by Era-NET NanoSci LECSIN project coordinated by F. Priolo, by the Italian Ministry of University and Research, and the UK EPSRC UK Silicon Photonics project. The fabrication was carried out in the framework of NanoPiX (see http://www.nanophotonics.eu).